Functional ESCRT machinery is required for constitutive recycling of claudin-1 and maintenance of polarity in vertebrate epithelial cells

Joseph D. Dukes*, Laura Fish*, Judith D. Richardson, Elizabeth Blaikley, Samir Burns, Christopher J. Caunt, Andrew D. Chalmers†, and Paul Whitley†
Department of Biology and Biochemistry, Centre for Regenerative Medicine, University of Bath, Bath BA2 7AY, United Kingdom

ABSTRACT **Genetic screens in *Drosophila* have identified regulators of endocytic trafficking as neoplastic tumor suppressor genes. For example, *Drosophila* endosomal sorting complex required for transport (ESCRT) mutants lose epithelial polarity and show increased cell proliferation, suggesting that ESCRT proteins could function as tumor suppressors. In this study, we show for the for the first time to our knowledge that ESCRT proteins are required to maintain polarity in mammalian epithelial cells. Inhibition of ESCRT function caused the tight junction protein claudin-1 to accumulate in intracellular vesicles. In contrast E-cadherin and occludin localization was unaffected. We investigated the cause of this accumulation and show that claudin-1 is constitutively recycled in kidney, colon, and lung epithelial cells, identifying claudin-1 recycling as a newly described feature of diverse epithelial cell types. This recycling requires ESCRT function, explaining the accumulation of intracellular claudin-1 when ESCRT function is inhibited. We further demonstrate that small interfering RNA knockdown of the ESCRT protein Tsg101 causes epithelial monolayers to lose their polarized organization and interferes with the establishment of a normal epithelial permeability barrier. ESCRT knockdown also reduces the formation of correctly polarized three-dimensional cysts. Thus, in mammalian epithelial cells, ESCRT function is required for claudin-1 trafficking and for epithelial cell polarity, supporting the hypothesis that ESCRT proteins function as tumor suppressors.**

Monitoring Editor
Asma Nusrat
Emory University

Received: Apr 20, 2011
Revised: Jun 16, 2011
Accepted: Jun 25, 2011

INTRODUCTION

Epithelial tissues are characterized by a polarized cellular architecture and specialized cell–cell junctions. These include desmosomes and adherens junctions that mediate cell adhesion and tight junctions that control paracellular movement of molecules across epithelial sheets (Getsios *et al.*, 2004; Shin *et al.*, 2006; Niessen and Gottardi, 2008). Each of these epithelial junctions consists of multiple proteins, for example, tight junctions contain transmembrane proteins, such as occludin and claudins, and membrane-associated proteins, such as ZO-1. The molecules responsible for recruiting these proteins into functional junctions and generating polarized tissues include a number of polarity complexes and signaling proteins (Suzuki and Ohno, 2006; Goldstein and Macara, 2007; Bryant and Mostov, 2008). Epithelial junctions, once established, are dynamic structures that are constantly being remodeled (Shen *et al.*, 2008; Steed *et al.*, 2010). Understanding the mechanisms responsible for the formation, maintenance, and remodeling of epithelial junctions is crucial, as alterations in cell junctions have been linked to a wide range of pathological conditions, such as cancer and inflammatory bowel diseases (Yang and Weinberg, 2008; Yu and Turner, 2008; Capaldo and Nusrat, 2009; Brennan *et al.*, 2010).

This article was published online ahead of print in MBoC in Press (http://www.molbiolcell.org/cgi/doi/10.1091/mbc.E11-04-0343) on July 20, 2011.

*These authors contributed equally to this work.

†These authors were co–principal investigators.

Address correspondence to: Andrew D. Chalmers (ac270@bath.ac.uk) or Paul Whitley (bssprw@bath.ac.uk).

Abbreviations used: EGFR, epidermal growth factor receptor; ESCRT, endosomal sorting complex required for transport; FBS, fetal bovine serum; GFP, green fluorescent protein; LDLR, low-density lipoprotein receptor; M6PR, mannose-6-phosphate receptor; MESNA, 2-mercaptoethanesulfonate; PBS, phosphate-buffered saline; PFA, paraformaldehyde fixation buffer; siRNA, small interfering RNA; TER, transepithelial resistance; TfR, transferrin receptor.

There is growing evidence of links among endocytosis, regulation of epithelial junctions (Ivanov *et al.*, 2005), and cell polarity (Shivas *et al.*, 2010). For example, mutants in *Drosophila* endosomal sorting complex required for transport (ESCRT) machinery components lose epithelial cell polarity and show a dramatic tissue overgrowth phenotype (Moberg *et al.*, 2005; Thompson *et al.*, 2005; Vaccari and Bilder, 2005, 2009; Herz *et al.*, 2006, 2009; Rodahl *et al.*, 2009; Vaccari *et al.*, 2009). The ESCRT machinery is conserved from yeast to mammals and is made up of ESCRT-0, -I, -II, and -III subcomplexes, each consisting of multiple ESCRT proteins. These proteins have a well-established role in the trafficking of ubiquitylated transmembrane proteins to lysosomes for degradation (Hurley and Emr, 2006; Raiborg and Stenmark, 2009). They are believed to function in the selection of cargo, invagination of endosome membranes, and scission of the invaginations to form intraluminal vesicles (Hurley and Emr, 2006; Raiborg and Stenmark, 2009). This pathway is important for attenuating signaling from growth factor receptors, such as the epidermal growth factor receptor (EGFR; Malerod *et al.*, 2007). In addition to blocking the degradative pathway, inhibition of ESCRT function has been reported to cause defects in the recycling of transmembrane proteins (Yoshimori *et al.*, 2000; Fujita *et al.*, 2003; Doyotte *et al.*, 2005; Baldys and Raymond, 2009). These effects may be due to a loss of endosomal domain organization, caused by inhibition of the degradative pathway (Woodman, 2009), and suggest an interdependence between different endocytic trafficking routes. However, a requirement for ESCRT proteins in recycling to the plasma membrane is controversial, as other studies report that inhibiting ESCRT function causes an increase or has no effect on recycling (Babst *et al.*, 2000; Razi and Futter, 2006; Raiborg *et al.*, 2008). Finally, ESCRT proteins are involved in other processes requiring membrane fission, such as cytokinesis, autophagy, and viral budding (Garrus *et al.*, 2001; Martin-Serrano *et al.*, 2003; Zamborlini *et al.*, 2006; Carlton and Martin-Serrano, 2007; Rusten *et al.*, 2007; Dukes *et al.*, 2008). The striking loss of polarity and overgrowth phenotypes seen in *Drosophila* ESCRT mutants suggests that ESCRT proteins could act as tumor suppressors. However, although the ESCRT pathway has been linked to stimulus-induced degradation of cell adhesion and junction proteins (Palacios *et al.*, 2005; Leithe *et al.*, 2009; Lobert *et al.*, 2010), a role, if any, for the ESCRT proteins in maintaining epithelial polarity in vertebrates has not been determined.

In this study, we investigate for the first time to our knowledge whether ESCRT protein function is required for epithelial cell polarity and junction formation in mammalian epithelial cells. We show that the tight junction protein claudin-1 accumulated on intracellular vesicles after inhibition of ESCRT function in epithelial cell lines, while the localization of E-cadherin, occludin, and ZO-1 appeared normal. We investigated the possible causes of the intracellular accumulation, and found claudin-1 is constantly endocytosed and recycled back to the plasma membrane in different epithelial cell types. This recycling requires ESCRT function, explaining the accumulation of intracellular claudin-1 when ESCRT function is inhibited. We further demonstrate that the ESCRT protein Tsg101 is required for maintaining a polarized monolayer in human epithelial cells and for the establishment of a normal epithelial permeability barrier. Finally, we show that Tsg101 is required for correct formation of three-dimensional cysts. Thus ESCRT function is required for the recycling of claudin-1 and maintenance of polarity in mammalian epithelial cells.

RESULTS

ESCRT function is required for the correct localization of claudin-1 in epithelial cells

To investigate whether perturbation of ESCRT function affects cell polarity in vertebrate epithelial cells, we used two dominant negative ESCRT constructs. The first was a CHMP3$^{1–179}$GFP construct that has the C-terminal autoinhibitory domain removed (Whitley *et al.*, 2003; Zamborlini *et al.*, 2006; Shim *et al.*, 2007). CHMP3$^{1–179}$-green fluorescent protein (CHMP3$^{1–179}$GFP) was expressed in MDCK cells, a canine kidney cell line commonly used to study epithelial polarity. CHMP3$^{1–179}$GFP accumulated on intracellular vesicular structures (Figure 1), a phenotype similar to that observed in other cell lines (Dukes *et al.*, 2008). The tight junction proteins occludin and ZO-1 and the adherens junction protein E-cadherin showed the same localization in CHMP3$^{1–179}$GFP-expressing cells as control cells (Figure 1, A–C). The apical marker GP135/podocalyxin and the basolateral marker numb were also correctly localized (Figure S1A). However, the localization of claudin-1 was markedly different in CHMP3$^{1–179}$GFP-expressing cells in comparison to adjacent nontransfected cells (Figure 1D). Control cells contained small amounts of internal claudin-1, but levels of intracellular claudin-1 were greatly increased in CHMP3$^{1–179}$GFP-expressing cells (Figure 1D, arrowhead in Z-projection). A similar phenotype was also seen with claudin-2 (Figure S7A). Despite the intracellular accumulation of claudin-1, some remained at the junctions and along the lateral membrane (Figure 1D), as seen in nontransfected cells. The additional intracellular claudin-1 accumulated in large vesicular structures, and there was extensive colocalization between the internal claudin-1 and the dominant negative CHMP3$^{1–179}$GFP compartment (Figures 1D and S1B). Claudin-1 distribution was not affected by the expression of GFP alone (Figure 1E).

The second dominant negative mutant used was a GFP-tagged ATPase-defective Vps4 construct, GFP-Vps4^{E235Q} (Bishop and Woodman, 2000; Whitley *et al.*, 2003). Similar to the phenotype produced by expressing CHMP3$^{1–179}$GFP, this construct resulted in the accumulation of GFP-Vps4^{E235Q} and claudin-1 on large vesicular compartments when expressed in MDCK cells (Figure S2B). The cellular distribution of ZO-1 was indistinguishable from nonexpressing cells, localizing almost exclusively to cell surface junctions (Figure S2A). Claudin-1 distribution was unchanged after expression of a GFP-Vps4^{wt} control construct that does not alter endosomal trafficking (Figure S2C).

To assess whether the requirement of ESCRT function for the junctional localization of claudin-1 is specific to kidney-derived MDCK cells, we investigated the distribution of junction proteins in the human colon cancer–derived CaCo-2 cell line. Inhibition of ESCRT function with CHMP3$^{1–179}$GFP produced the same phenotype as seen in MDCK cells, an increase in intracellular claudin-1 (Figure S3A) and normal occludin, E-cadherin, and ZO-1 localization (Figure S3, B–D).

Internal claudin-1 and CHMP3$^{1–179}$GFP partially colocalize with ubiquitin and the transferrin receptor

To establish the identity of the CHMP3$^{1–179}$GFP/claudin-1–positive intracellular vesicles, we examined the localization of ubiquitin and a range of markers for endomembrane compartments. There was a dramatic increase in the amount of ubiquitin-positive structures in CHMP3$^{1–179}$GFP-transfected cells in comparison to nontransfected cells (Figure 2A), consistent with our previous work in Cos-7 and HeLa cells (Dukes *et al.*, 2008). Accumulation of ubiquitin is also seen in *Drosophila* ESCRT mutants (Moberg *et al.*, 2005; Thompson *et al.*, 2005; Vaccari and Bilder, 2005, 2009; Herz *et al.*, 2006, 2009;

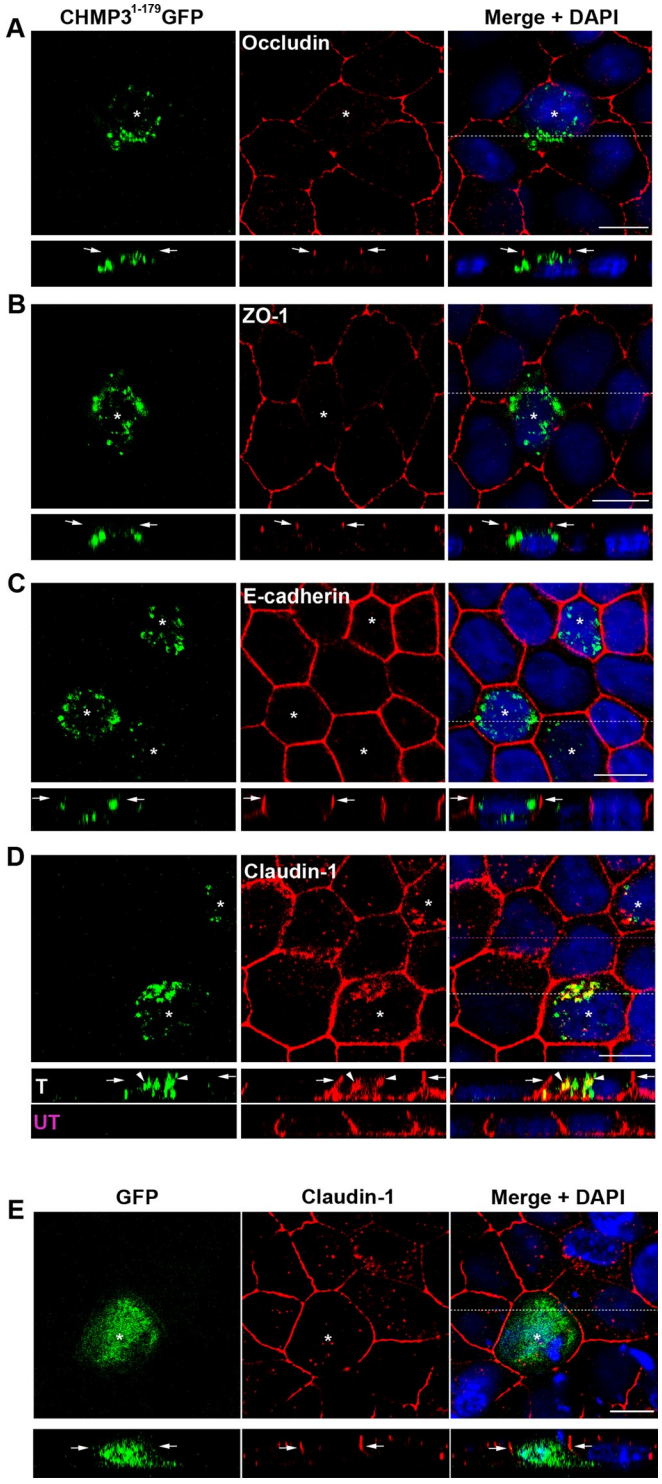

FIGURE 1: Perturbing ESCRT function in MDCK cells results in an intracellular accumulation of claudin-1. CHMP3$^{1–179}$GFP-expressingMDCK cells were stained with antibodies against: (A) occludin, (B) ZO-1, (C) E-cadherin, and (D) claudin-1. Claudin-1 accumulates intracellularly and extensively overlaps with the CHMP3$^{1–179}$GFP compartment. Z-sections are displayed below each of the panels and arrows indicate junctional region of CHMP3$^{1–179}$GFP-expressing cells (*). Arrowheads show internal overlap of claudin-1 and CHMP3$^{1–179}$GFP. Antibody staining (red) and CHMP3$^{1–179}$GFP (green) are shown together with merged images and DAPI (blue; right panels). (E) GFP (green)-expressing cells (marked with a *) were stained with antibodies against claudin-1 (red). Dotted lines show position of Z-projections. Scale bar: 10 μm.

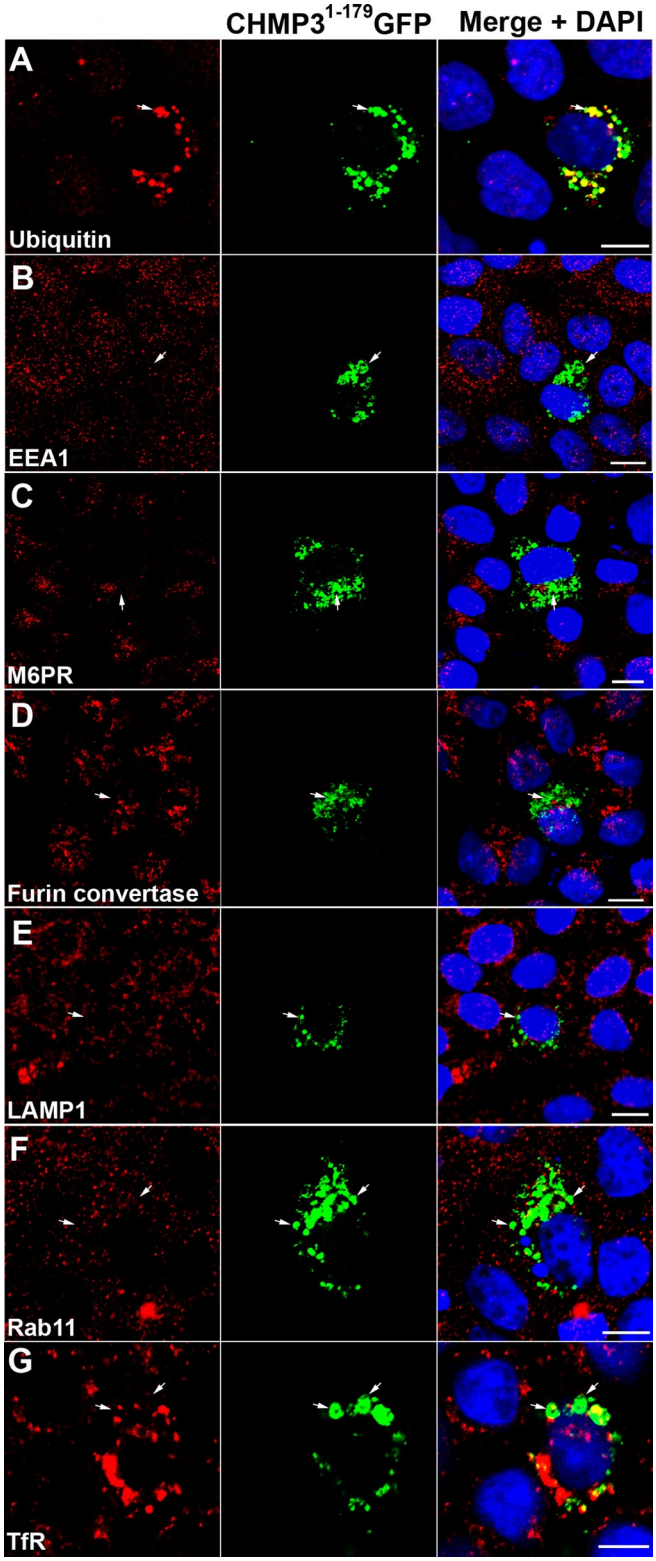

FIGURE 2: Perturbing ESCRT function in MDCK cells results in ubiquitin and TfR accumulation. CHMP3$^{1–179}$GFP-expressing MDCK cells were stained with antibodies against: (A) ubiquitin, (B) EEA-1 (early endosomes), (C) M6PR (late endosomes), (D) furin convertase (TGN), (E) LAMP-1 (lysosomes), (F) Rab11 (recycling endosomes), and (G) TfR (a recycled protein). Expression of CHMP3$^{1–179}$GFP caused accumulation of ubiquitin and TfR. The distribution of the other markers was unchanged. Antibody staining (red), CHMP3$^{1–179}$GFP (green), and nuclei stained with DAPI (blue) are shown together with merged images (right panels). Scale bar: 10 μm.

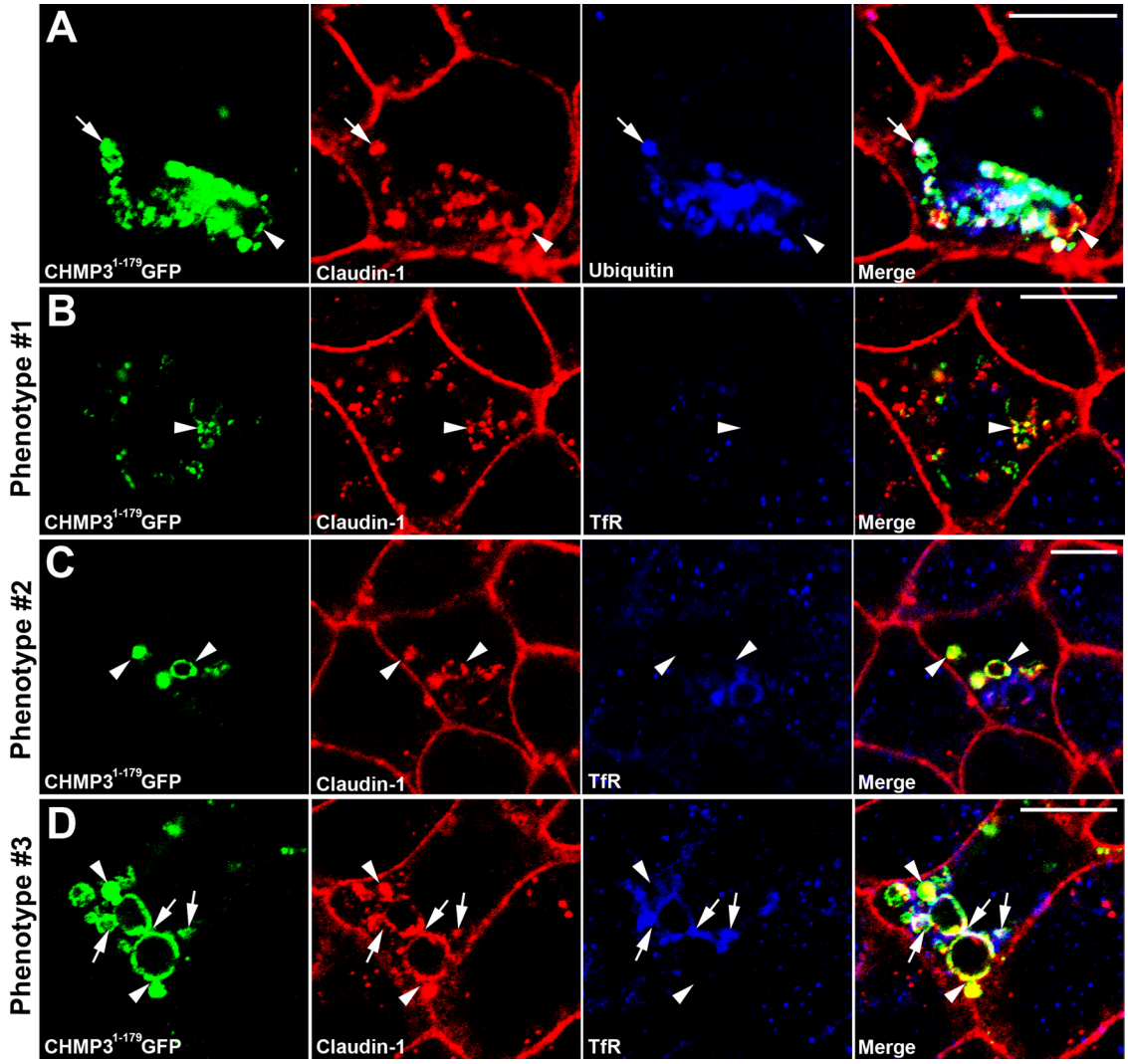

FIGURE 3: The accumulated intracellular claudin-1 partially colocalizes with ubiquitin and TfR. CHMP3$^{1–179}$GFP-expressing MDCK cells were stained with antibodies against: (A) ubiquitin and (B–D) TfR. CHMP3$^{1–179}$GFP, claudin-1, and ubiquitin/TfR show an overlapping distribution in some regions (arrows), but colocalization is not complete (arrowheads). The TfR distribution seems to be dependent on the level of expression of CHMP3$^{1–179}$GFP, as illustrated by the differing phenotypes. CHMP3$^{1–179}$GFP (green), claudin-1 (red), and ubiquitin/TfR (blue) are shown with merged images (far right panels). Scale bar: 10 μm.

Rodahl *et al.*, 2009; Vaccari *et al.*, 2009). The ubiquitin partially colocalized with the CHMP3$^{1–179}$GFP (Figure 2A) and triple labeling showed partial colocalization among CHMP3$^{1–179}$GFP, claudin-1, and ubiquitin (Figure 3A, arrow). This suggests that the dominant negative mutant is altering the flux of ubiquitylated proteins through the endocytic system. Intriguingly, the dominant negative did not markedly alter the distribution of the early endosomal marker EEA1, the late endosomal marker mannose-6-phosphate receptor (M6PR), the *trans*-Golgi network marker furin convertase, the lysosomal marker LAMP1, or the apical recycling endosome marker Rab11 (Figure 2, B–F). There was also no significant colocalization between the dominant negative compartment and these markers. This is in contrast to previous work in nonpolarized Cos-7 and HeLa cells, where early and late endosomal markers colocalized to the same compartment as CHMP3$^{1–179}$GFP (Dukes *et al.*, 2008). In polarized MDCK cells, transferrin is proposed to traffic through common recycling endosomes (Leung *et al.*, 2000) and, interestingly, the transferrin receptor (TfR) accumulated in CHMP3$^{1–179}$GFP-expressing cells (Figure 2G). Low levels of CHMP3$^{1–179}$GFP, which still caused claudin-1 accumulation, did not cause TfR accumulation (Figure 3B), but cells with higher levels of CHMP3$^{1–179}$GFP showed accumulation of TfR (Figure 3, C and D). The intracellular TfR partially colocalized with CHMP3$^{1–179}$GFP and the intracellular claudin-1 (Figure 3D, arrow). These results show that inhibiting ESCRT function in vertebrate epithelial cells does not alter the localization of several markers of endomembranes, but does cause the accumulation of intracellular ubiquitin and TfR, both of which partially colocalize with the intracellular claudin-1.

Claudin-1 is continually endocytosed and recycled to the cell surface in diverse epithelial cell types

Inhibition of ESCRT function leads to intracellular accumulation of claudin-1 (Figures 1 and 3) and ESCRT function is required for the degradation of selected membrane proteins (Raiborg and Stenmark, 2009). Therefore an inability of claudin-1 to be trafficked to lysosomes for degradation could explain its intracellular

accumulation. However, perturbation of ESCRT function may also inhibit the recycling of transmembrane proteins and other endosomal sorting events (Yoshimori *et al.*, 2000; Fujita *et al.*, 2003; Doyotte *et al.*, 2005; Baldys and Raymond, 2009). The intracellular claudin-1 also partially colocalizes with TfR, which is a recycled cargo. Thus intracellular accumulation of claudin-1 could be a result of inhibiting endocytic recycling.

To investigate the trafficking of claudin-1 and occludin in MDCK cells, we used a surface biotinylation assay. Surface claudin-1 and occludin were detected after labeling with a membrane-impermeant biotin label (Figure S4A, surface biotin) but not in pulldowns from mock treated cells, demonstrating that the pulldown is specific to biotinylated proteins (Figure S4A, nonspecific). The biotin was also efficiently removed from labeled proteins by surface stripping (Figure S4A, strip control). For the endocytosis assay (Figure S4B), surface proteins on MDCK cells were labeled at 4°C. Following this, the cells were placed at 37°C to allow trafficking, biotin was stripped from surface proteins, and analysis of the remaining biotinylated proteins was performed. Only those proteins that are surface-labeled and then endocytosed will be resistant to surface stripping. Following a 60-min incubation at 37°C, ~35% of the biotinylated claudin-1 was resistant to surface stripping, showing that a significant amount of claudin-1 is endocytosed (Figure S4B, "Endocytosis 60 min"). The endocytosis is rapid as the amount of internal claudin-1 reached a plateau by 30 min (Figure S4C). Biotinylated occludin resistant to surface stripping could not be detected (Figure S4B, "Endocytosis 60 min"), suggesting that in MDCK cells occludin is not endocytosed in this time frame.

The fate of the endocytosed claudin-1 was then investigated. MDCK cells were labeled as described in the preceding paragraph and incubated at 37°C for 1 h to allow endocytosis. Cells were surface-stripped of biotin and incubated again at 37°C for 20 min. Following this second 37°C incubation, cells were surface-stripped for a second time or mock-treated. The second stripping removes biotin from endocytosed proteins that have returned to the cell surface, so recycling would be shown by a reduction in signal in the recycling lane relative to the degradation control. This revealed that the majority of internalized claudin-1 returns to the cell surface (Figure 4A, "Recycling 20 min"). When cells were incubated for the second time but not stripped, there was no reduction in levels of biotinylated claudin-1 (Figure 4A, "Degradation control"). This is an important result that demonstrates the loss of biotinylated claudin-1 is not because it is targeted for degradation. The biotinylation assays demonstrate that claudin-1, but not occludin, is constantly endocytosed and then recycled back to the plasma membrane in MDCK cells. It is possible that this dynamic endocytosis and recycling of claudin-1 occurs in cells that have just reached confluency, but not in more mature monolayers. Recycling of claudin-1 was therefore investigated in MDCK cells that had been confluent for 10 d rather than 3 d. No difference in the amount of endocytosis or recycling was observed in MDCK cells with the more mature junctions (Figure S4D). The surface biotinylation assay also confirmed that TfR is endocytosed and recycled (Figure S4E) as expected (Leung *et al.*, 2000).

To establish whether claudin-1 recycling is a common feature of epithelial cells, we performed the biotinylation assay on CaCo-2 cells and 16-HBE cells, a human bronchial epithelial cell line (Figure 4, B and C). The results show that claudin-1 is continuously endocytosed and recycled in both of these cell types, with only a very small proportion of claudin-1 being targeted for degradation (Figure 4, B and C). However, whereas endocytosis of occludin was not observed in the MDCK cells, ~40% of surface-labeled occludin was internal in CaCo-2 and 16-HBE cells following 60 min of incubation at 37°C. In these cell lines, the fate of internalized occludin was split between degradation and recycling back to the plasma membrane (Figure 4, B and C). To summarize, claudin-1 is endocytosed and recycled in all cell lines tested. This is in contrast to occludin that is endocytosed, then degraded or recycled in CaCo-2 and 16-HBE cells, but not endocytosed in MDCK cells.

ESCRT function is required for the continuous recycling of claudin-1

The demonstration that claudin-1 is continually recycled suggests a block in recycling could cause the intracellular accumulation of claudin-1 seen in cells expressing dominant negative ESCRT proteins. Testing this hypothesis with the biochemical assay requires that the dominant negative be expressed in a high percentage of cells. To achieve this, we used an adenovirus system, which gave expression in virtually all cells (Figure 5A). Expressing the CHMP3$^{1–179}$GFP protein caused a striking inhibition of claudin-1 recycling, from 65% of the endocytosed protein in controls to just 4% in CHMP3$^{1–179}$GFP adenovirus-infected cells (Figure 5, B and C). There was also an increase in the amount of endocytosed protein and a reduction in surface claudin-1 (Figure 5, C and D). Consistent with the accumulation of TfR seen after expressing CHMP3$^{1–179}$GFP, the recycling of TfR was also inhibited (Figure S5). This shows for the first time to our knowledge that ESCRT function is required for the recycling of claudin-1.

Tsg101 is required to maintain a polarized single-layered epithelial barrier

The dominant negative ESCRT experiments showed ESCRT function is required for the recycling of claudin-1, but it remained to be established whether ESCRT function is required to maintain epithelial polarity in vertebrates as it is in *Drosophila*. To study the requirement of ESCRT proteins in maintaining polarity, we used small interfering RNA (siRNA) knockdown of the ESCRT-I protein Tsg101. This protein was chosen because it was initially identified as a potential tumor suppressor in mammalian cells (Li and Cohen, 1996), and it was one of the first ESCRT proteins shown to be required for polarity in *Drosophila* (Moberg *et al.*, 2005). CaCo-2 cells, rather than MDCK cells, were used due to the availability of siRNA reagents for human genes.

Efficient knockdown of Tsg101 was confirmed by immunoblotting (Figure 6A), and analysis of the resulting phenotype demonstrated there were large areas where the cellular architecture appeared disrupted (Figure 6B, arrow). In these regions, the normal single-layered organization was lost, and multilayered stacks of cells formed (Figure 6C). In other areas, the cells appeared to maintain their normal monolayered organization (Figure 6B, arrowhead).

Analysis of junction and polarity markers in Tsg101 knockdown cells showed that accumulation of internal claudin-1, partially colocalized with ubiquitin, was observed in regions that maintained monolayer organization (Figure 6D). Intracellular claudin-4 also accumulated (Figure S7B). In contrast, there did not appear to be any internal accumulation or disruption of desmoglein 2 (a desmosome marker), occludin, E-cadherin, or ZO-1 (Figure S6). This phenotype is consistent with results using the dominant negative ESCRT constructs. However, in the multilayered regions formed after Tsg101 knockdown, a much more pronounced polarity defect was observed. In these regions, correct apicobasal polarity was disrupted, and many cells were incorrectly oriented relative to the epithelial sheet (Figure 7). To establish if Tsg101 knockdown had a functional impact on epithelial barrier formation, transepithelial resistance (TER) was monitored. Tsg101 knockdown significantly reduced TER compared with control at all time points measured (Figure 8A),

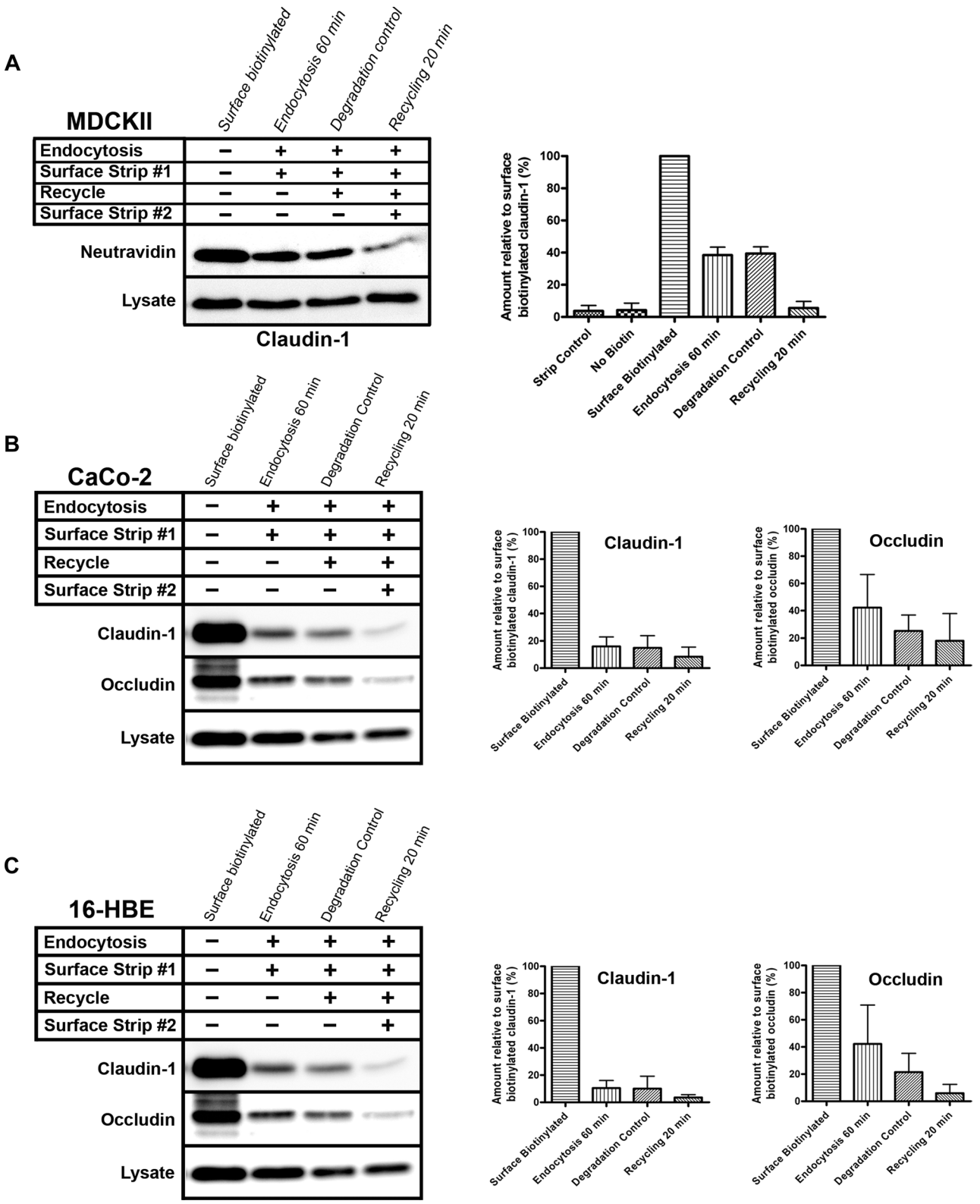

FIGURE 4: Claudin-1 is constitutively endocytosed and recycled back to the plasma membrane in different epithelial cell types. The surface biotinylation, endocytosis, and recycling assay was performed on: (A) MDCK cells, (B) CaCo-2 cells, and (C) 16-HBE cells. Lanes marked "Surface biotinylated" represent the initial biotinylated protein at the cell surface; "Endocytosis 60 min" is the internal biotinylated protein that is resistant to surface stripping. Degradation is shown by a reduction of signal in the "Degradation control" lane in comparison to the "Endocytosis 60 min" lane. Recycling is the reduction of signal in the "Recycling 20 min" lane relative to the "Degradation control" lane. The data shown graphically are the means ± SD from four independent experiments.

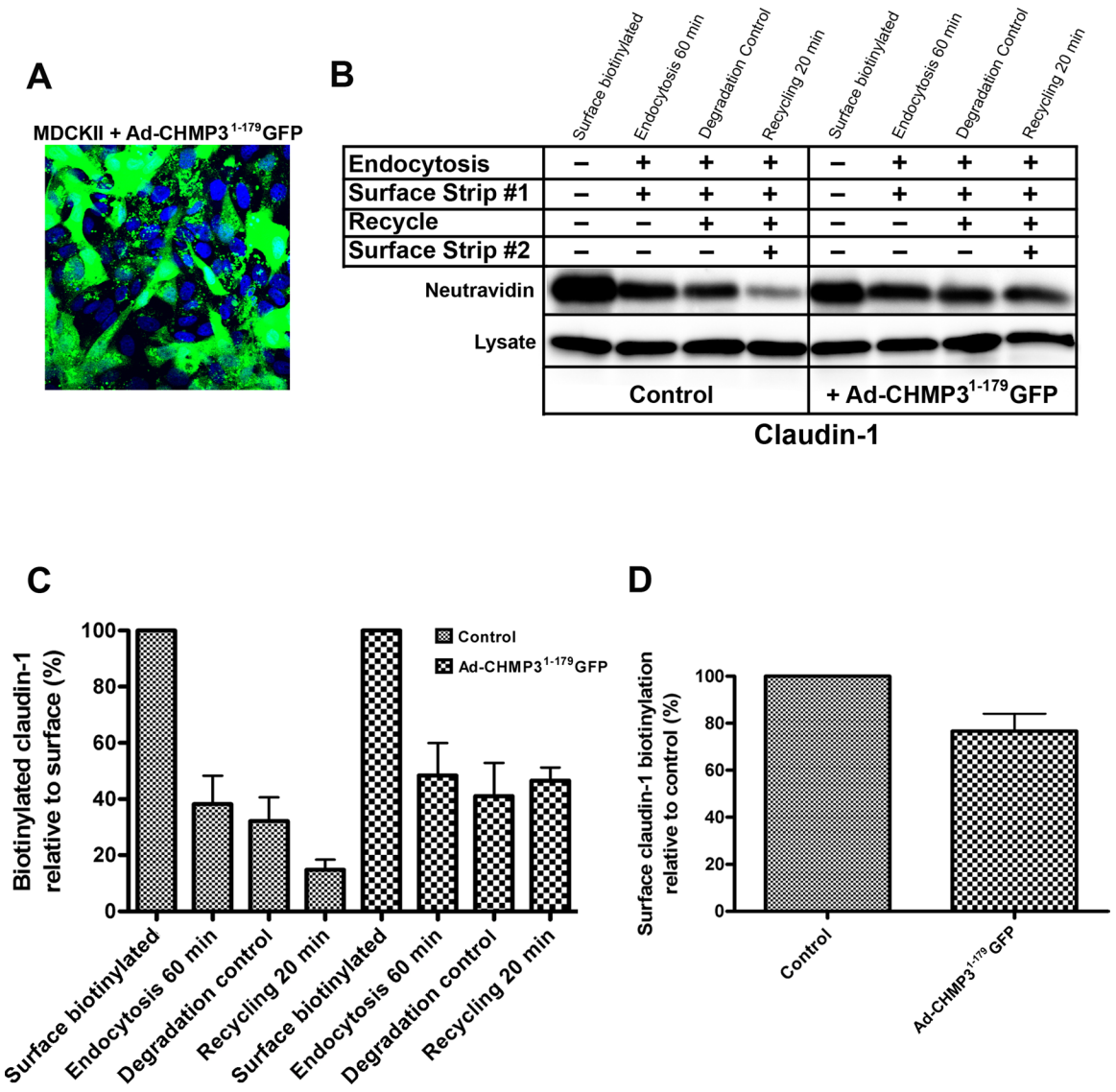

FIGURE 5: ESCRT function is required for the normal recycling of claudin-1 in MDCK cells. (A) Infection of MDCK cells with Ad-CHMP3$^{1–179}$GFP resulted in most cells expressing the protein; CHMP3$^{1–179}$GFP (green) and nuclei (blue). (B and C) Cells were either mock-treated (left blot) or infected with Ad-CHMP3$^{1–179}$GFP (right blot) for 16 h, after which the biotin endocytosis and recycling assay were performed. The data shown graphically are the means ± SD from three independent experiments. In Ad-CHMP3$^{1–179}$GFP–treated cells, there is no significant reduction in the "Recycling 20 min" lane, indicating that claudin-1 is not recycled. (D) Quantification of surface-biotinylated claudin-1 showed a reduction in Ad-CHMP3$^{1–179}$GFP–infected cells.

demonstrating that Tsg101 is required for epithelial cells to form a tight diffusion barrier across an epithelial sheet.

Tsg101 knockdown interferes with the polarization of three-dimensional cysts

Three-dimensional cultures are considered a more physiologically relevant way of investigating cell polarity in vitro (Martin-Belmonte and Mostov, 2008). We therefore used a three-dimensional epithelial cyst formation assay to further investigate the role of ESCRT proteins in regulating epithelial cell polarity. CaCo-2 cells treated with nontargeting siRNA developed into cysts with a single central lumen in 64% of cases (Figure 8B). Remaining cysts failed to develop a lumen or formed epithelial balls containing multiple small cavities. However, upon depletion of Tsg101, CaCo-2 cells formed cysts with a single lumen in only 42% of cases, and the proportion of multilumen cysts doubled (Figure 8B). In summary, these results show that Tsg101 is required for correct epithelial polarity in both two-dimensional and three-dimensional CaCo-2 cell cultures.

DISCUSSION

In this study, the consequences of perturbing ESCRT function on the polarity of vertebrate epithelial cells were investigated for the first time to our knowledge. Our data demonstrate that inhibiting ESCRT function with dominant negative constructs or siRNA knockdown causes accumulation of internal claudin-1. The biotinylation assays show claudin-1 is constitutively recycled in epithelial cells, and ESCRT function is required for this recycling. Therefore the accumulation of claudin-1 in ESCRT-deficient cells can be attributed to a block in this recycling pathway. Finally, the ESCRT protein Tsg101 is shown to be required for maintenance of polarity and establishment of a permeability barrier in epithelial sheets, as well as for epithelial cells to correctly polarize in three-dimensional

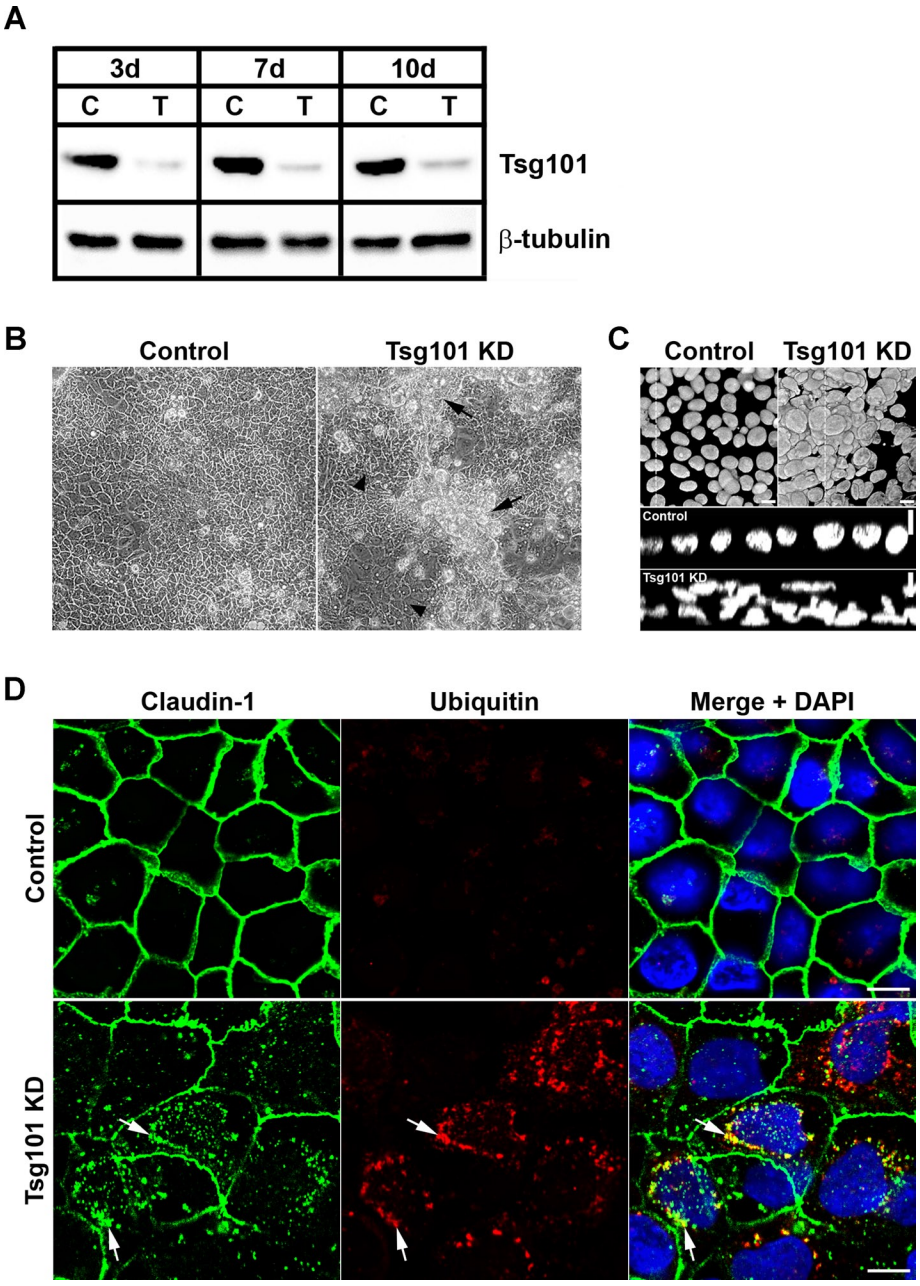

FIGURE 6: siRNA knockdown of Tsg101 disrupts epithelial monolayer organization and causes internal accumulation of claudin-1 and ubiquitin in CaCo-2 cells. (A) CaCo-2 cells were transfected with either ON-TARGETplus Non-targeting siRNA ("C") or Tsg101 siRNA ("T") and incubated for 3, 7, and 10 d, after which lysates were immunoblotted for Tsg101 and β-tubulin as a loading control. (B) CaCo-2 cells were transfected with either ON-TARGETplus Non-targeting siRNA or Tsg101 siRNA and analyzed via light microscopy after 7 d. Tsg101 knockdown cells form monolayers in some areas (arrowheads), but many regions are observed where epithelial organization appears disrupted (arrows). (C) Nuclei of knockdown cells stained with DAPI. Tsg101 knockdown disrupts cellular architecture and regions of cells show a multilayered organization. (D) After a 7-d knockdown, cells were stained for claudin-1 (green) and ubiquitin (red). Knockdown of Tsg101 resulted in increased levels of internal claudin-1 and ubiquitin. There was some overlap between them (arrows). Images in (D) are from regions of the knockdown where monolayered organization was maintained; a more striking polarity phenotype is seen in the multilayered regions (Figure 7). Merged images with nuclei stained with DAPI (blue) are shown. Scale bar: 10 μm.

cultures. Thus ESCRT function is required for the recycling of a key junction protein and for the correct polarization of vertebrate epithelial cells.

Claudin-1 recycling is a feature of diverse epithelial cell types

Claudins are crucial for producing a tight junction permeability barrier (Van Itallie and Anderson, 2006), which makes understanding the processes regulating localization of claudin proteins central to tight junction biology. Endocytosis of claudins can occur in epithelial cells by a peculiar mechanism involving internalization of plasma membrane from juxtaposed cells (Matsuda *et al.*, 2004) and expression of the ubiquitin ligase LNX1p80 drives endocytosis and degradation of claudin-1 (Takahashi *et al.*, 2009). Our data demonstrate that internalized claudin-1 in unstimulated epithelial monolayers is constitutively and rapidly recycled back to the plasma membrane. We did not detect significant degradation of claudin-1 over the time frame of our assays (minutes), but previous work has shown that over longer time periods (hours/days) claudin-1 is degraded (Takahashi *et al.*, 2009). We propose that, while the majority of endocytosed claudin-1 is recycled, a small percentage is selected for degradation, producing a gradual turnover of claudin-1 in MDCK cells.

Claudin-1 is located in the lateral membrane, as are the junctional complexes of polarized epithelial cells (Rahner *et al.*, 2001; Van Itallie *et al.*, 2003; Vogelmann and Nelson, 2005). Both of these pools are still present in cells expressing CHMP3$^{1–179}$GFP, and we see no evidence of selective depletion of a particular pool. However, as a mobile fraction of claudin-1 exists in tight junctions (Shen *et al.*, 2008), there may well be exchange between lateral and junctional pools of claudin-1. Depletion of one would then cause an indirect depletion of the other pool. This means an effect on a particular pool is likely to be difficult to observe.

This work focuses on claudin-1, but we must mention that we noted that in addition to the accumulation of claudin-1 there was accumulation of claudin-2 in CHMP3$^{1–179}$GFP-expressing MDCK cells and claudin-4 in Tsg101 knockdown CaCo-2 cells (Figure S7), suggesting that these claudins may also show ESCRT-dependent recycling. However, there are many examples of individual claudins showing different behaviors, for example, occludin dephosphorylation enhances exchange of junctional claudin-1 and claudin-2, but not claudin-4 (Raleigh *et al.*, 2011), while EGF stimulation induces degradation of claudin-2, but not claudin-1 (Ikari *et al.*, 2010), so a thorough analysis of the trafficking of different claudin family members is required to establish whether they undergo ESCRT-dependent recycling.

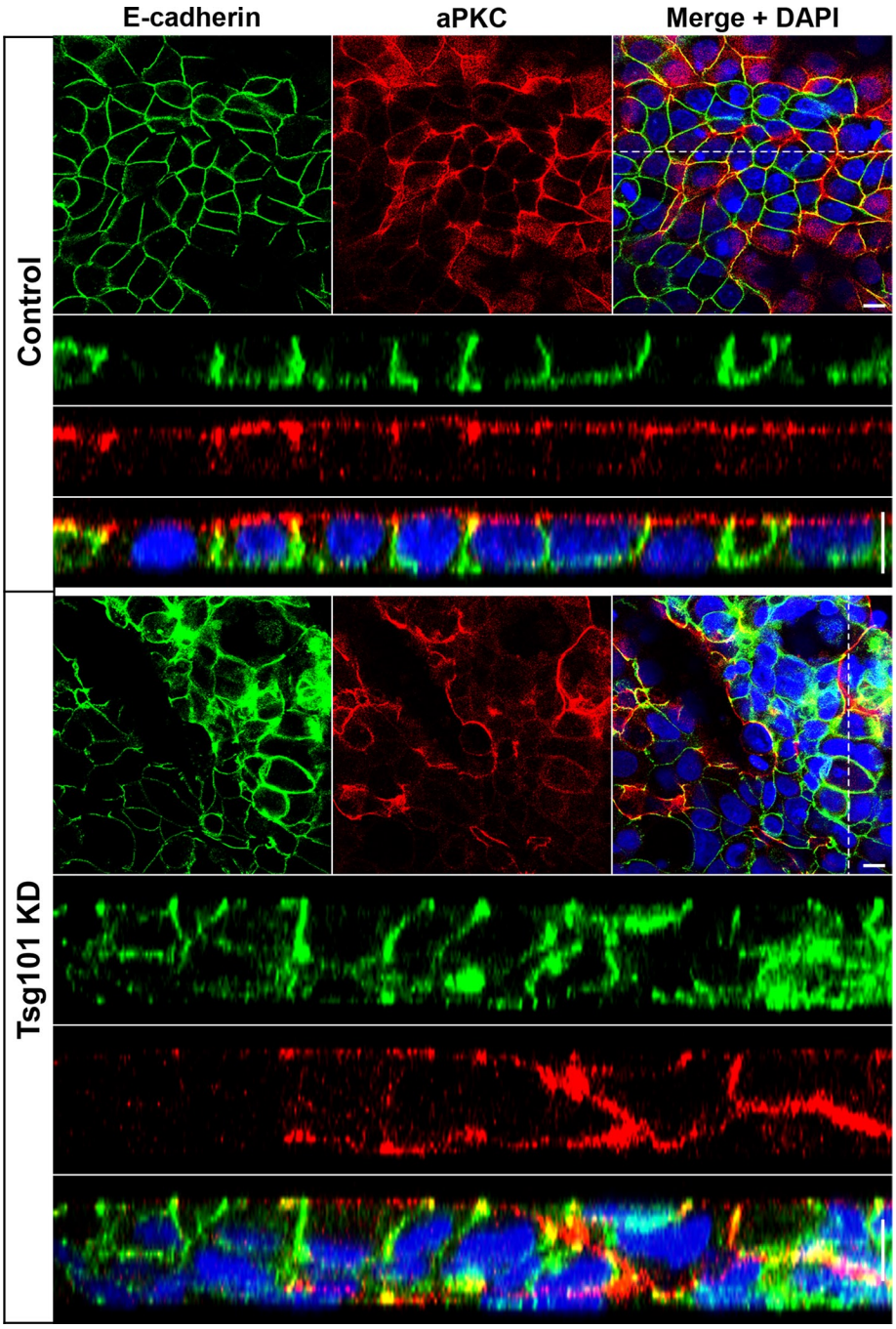

FIGURE 7: Tsg101 is required to maintain a polarized epithelial monolayer in CaCo-2 cells. CaCo-2 cells were transfected with either ON-TARGETplus Non-targeting siRNA or Tsg101 siRNA, incubated for 7 d, and stained for E-cadherin (green) and aPKC (red) to visualize basolateral and apical surfaces, respectively. Tsg101 knockdown cells form multilayered regions with compromised apicobasal polarity. Nuclei were stained with DAPI (blue). Apical confocal slices and corresponding Z-sections (indicated by dotted line) are displayed. Scale bar: 10 μm.

The continuous recycling of claudin-1 adds an important element to our understanding of claudin trafficking and supports a model whereby stability of cell contacts in epithelial monolayers is maintained by a balance between disassembly and assembly of cell junctions (Shen and Turner, 2008). Disruption of tight junction protein recycling would tend to lead to weakening or perhaps disassembly of tight junctions. Therefore it is tempting to speculate that claudin recycling might be altered in the wide range of pathogenic states associated with altered epithelial junctions, such as cancer and inflammatory bowel diseases (Yang and Weinberg, 2008; Yu and Turner, 2008; Capaldo and Nusrat, 2009). This raises the issue of how this recycling is regulated. Our data show that ESCRT function is required for claudin-1 recycling. This is consistent with previous work showing that ESCRT function is required for the recycling of epidermal growth factor receptor (EGFR) and low-density lipoprotein receptor (LDLR; Yoshimori *et al.*, 2000; Fujita *et al.*, 2003; Doyotte *et al.*, 2005; Baldys and Raymond, 2009). The trafficking of internalized claudin-1 to the plasma membrane after a calcium switch requires Rab13 and its binding protein JRAB/MICAL-L2 (Yamamura *et al.*, 2008). Rab13 is also required for the continuous recycling of occludin in the mouse mammary epithelial line (MTD1a; Morimoto *et al.*, 2005), indicating that Rab13 may be required for our observations of the continuous recycling of claudin-1. Future work will need to study ESCRTs, Rabs, and other regulators of endocytic trafficking to establish how the recycling of claudin-1 is mediated.

Variation between the recycling of claudin-1 and occludin

A feature of this study is the differences seen between the trafficking of claudin-1 and occludin. Claudin-1 was recycled in kidney (MDCK), colon (CaCo-2), and lung (16-HBE) cell lines. In contrast, occludin was recycled and degraded in CaCo-2 and 16-HBE cells, while in MDCK cells it was not endocytosed over the time frame analyzed. Previous work has shown that in MTD1a cells, occludin is rapidly endocytosed and recycled to the plasma membrane, whereas claudin-1 is not (Morimoto *et al.*, 2005). It appears that there is cell type–specific variation in the trafficking of claudin-1 and occludin, so that in some cells types they are both undergoing rapid trafficking, while in others trafficking is restricted to one of these junction proteins.

Perturbing ESCRT function caused intracellular accumulation of claudin-1 but not occludin. In MDCK cells, low levels of occludin endocytosis may explain this difference. However, claudin-1 and occludin are both endocytosed in CaCo-2 cells, but only claudin-1 accumulates. There are a number of independent recycling pathways (Grant and Donaldson, 2009), and our data may indicate that claudin-1 is returned to the plasma membrane by a pathway requiring ESCRT function that is distinct from the pathway used to recycle occludin. Consistent with junctional proteins following independent endocytic trafficking routes is data showing that selective internalization of tight junction proteins occurs (Hopkins *et al.*, 2003; Yu and Turner, 2008). This internalization may be mediated by specific ubiquitin ligases, such as LNX1p80 for claudin-1 (Takahashi *et al.*, 2009), Itch for occludin (Traweger *et al.*, 2002), and Hakai for E-cadherin (Fujita

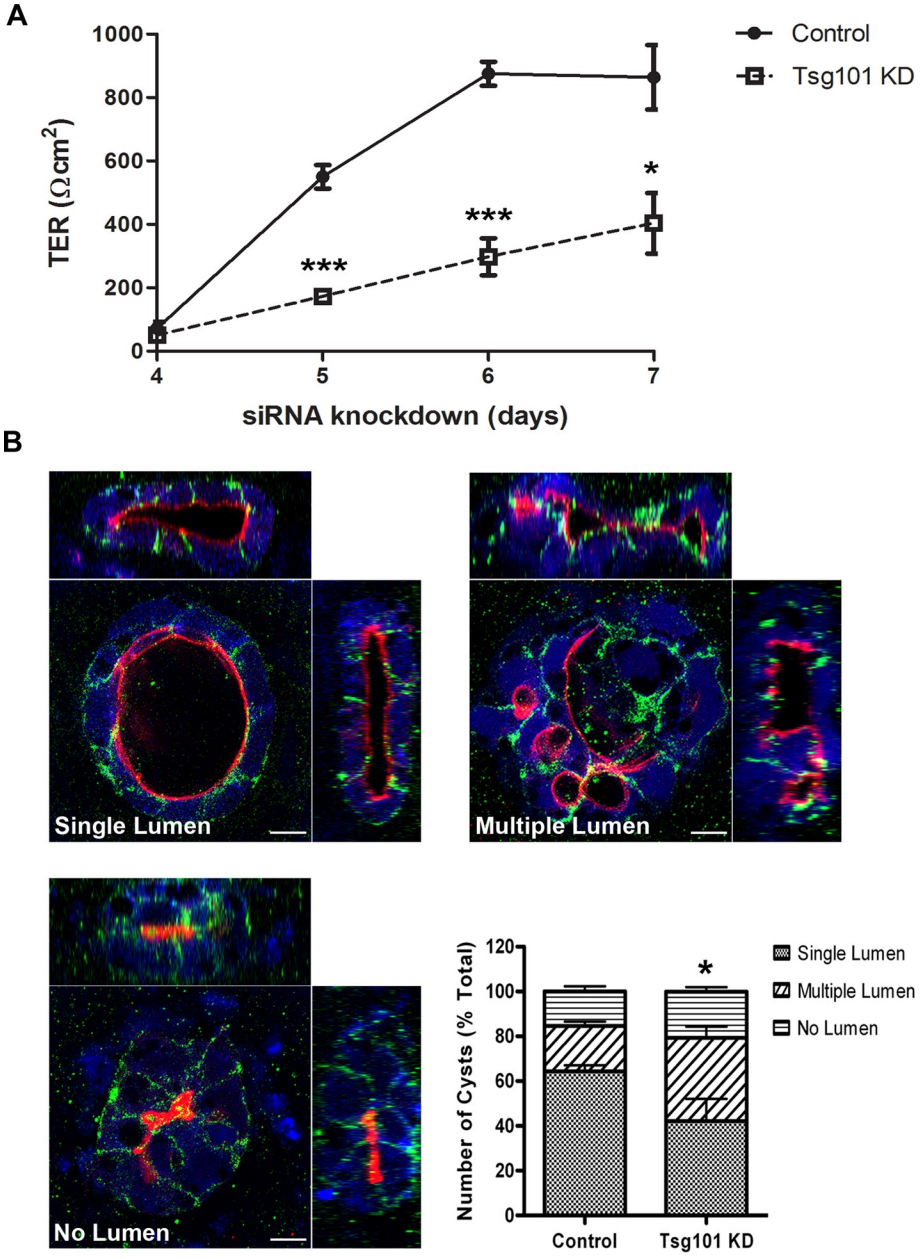

FIGURE 8: Tsg101 siRNA knockdown decreases TER and impairs formation of CaCo-2 three-dimensional cysts. (A) CaCo-2 cells were transfected with either ON-TARGETplus Non-targeting siRNA or Tsg101 siRNA, replated on day 3 to Transwell filters, and TER was measured between day 4 and day 7. (B) CaCo-2 cells were transfected with either ON-TARGETplus Non-targeting siRNA or Tsg101 siRNA, incubated for 3 d, and replated into a Matrigel suspension. Following incubation for 10 d, cysts were stained for aPKC (red) and E-cadherin (green) to mark the apical and basolateral membranes respectively. Nuclei were stained with DAPI (blue). Cysts display either a single lumen, multiple lumen, or no lumen. Z-sections are displayed for each cyst along with a confocal plane through the center. Scale bar: 10 μm. The number of cysts showing either single, multiple, or no lumen was quantified (bar graph). Data shown are the overall means from three independent experiments; >100 cysts were analyzed per condition for each experiment. Error bars represent SD. Results were analyzed using a *t* test, *** $p \leq 0.001$; * $p \leq 0.05$.

et al., 2002). Furthermore, in MDCK cells, E-cadherin returns to the plasma membrane via a Rab8-dependent route and tight junction proteins via a Rab13-dependent pathway (Yamamura *et al.*, 2008). It would be interesting to establish the mechanism underlying potential differences in trafficking routes of junctional proteins and to determine why there is variation across different cell types.

Junction recycling and loss of polarity

Individual ESCRT proteins are required to maintain polarity and prevent tissue overgrowth in *Drosophila* (Moberg *et al.*, 2005; Thompson *et al.*, 2005; Vaccari and Bilder, 2005, 2009; Herz *et al.*, 2006, 2009; Rodahl *et al.*, 2009; Vaccari *et al.*, 2009), and our data show that this requirement is conserved in vertebrate epithelial cells. It is currently not clear why ESCRT proteins are required to maintain polarity, but the widespread role of endocytic traffic in regulating signaling suggests that altered polarity signaling may be responsible (Vaccari and Bilder, 2009). On the basis of our results, we propose that a failure to return junctional proteins to the cell surface, where they normally function, provides an additional mechanism that might destabilize epithelial junctions and contribute to the loss of polarity. Simply inhibiting claudin-1 recycling is unlikely to explain the loss of polarity, as claudin-1 knockout mice have an epidermal defect but apparently do not experience a large-scale loss of epithelial polarity (Furuse *et al.*, 2002). However, epithelial cells contain many junctional proteins, and it seems possible the recycling of a number of these could require ESCRT function, so a loss of recycling combined with alterations in signaling might cause the loss of epithelial polarity.

ESCRTs as tumor suppressors

The reduced ability of ESCRT knockdown cells to polarize supports the hypothesis that ESCRT proteins could function as tumor suppressors in mammals. Previous work has shown that the ESCRT-I component VPS37A has reduced expression in hepatocellular carcinoma (Xu *et al.*, 2003), the ESCRT-III component CHMP1A has lower expression in pancreatic tumors (Li *et al.*, 2008), and knocking down the expression of CHMP1A in human pancreatic ductal tumor cells increases cell growth (Li *et al.*, 2008). However, mouse knockout studies have not supported a tumor suppressor function of ESCRT proteins (Ruland *et al.*, 2001; Wagner *et al.*, 2003), although it may be that apoptosis masks the tumorigenic potential, as is the case in *Drosophila* (Thompson *et al.*, 2005). There are also reports of increased expression of ESCRT proteins in tumors (Liu *et al.*, 2002; Oh *et al.*, 2007; Toyoshima *et al.*, 2007; Young *et al.*, 2007), and it has been suggested that the overexpressed protein may have a dominant negative effect (Vaccari and Bilder, 2009). In cancers with reduced ESCRT function, the cells may have increased signaling from growth factor receptors such as the EGFR (Malerod *et al.*, 2007). Our work shows that a reduction in ESCRT function in vertebrate epithelial cells promotes a loss of the normal polarized epithelial monolayer. Therefore loss of ESCRT function in cancer

cells could cause increased proliferation together with less stable tissue architecture, two of the key features acquired by tumor cells (Hanahan and Weinberg, 2000).

MATERIALS AND METHODS

Antibodies and DNA constructs

The DNA constructs CHMP3$^{1–179}$GFP, GFP-Vps4^{E235Q}, and GFP-Vps4^{WT} have been described previously (Whitley *et al.*, 2003; Dukes *et al.*, 2008), and the GFP construct used was pCS2-GFP (Chalmers *et al.*, 2006). Rabbit anti–claudin-1* (59–9000), mouse anti–claudin-2* (32–5600), mouse anti–claudin-4* (32–9400), rabbit anti-occludin (71–1500), mouse anti-occludin* (33–1500), mouse anti–ZO-1 (33–9100), mouse anti–E-cadherin (33–4000), mouse anti-TfR (13–6800), and rabbit anti-Rab11 (71–5300) were all purchased from Zymed (San Fransico, CA), and all used at a dilution of 1:25 for immunofluorescence and 1:1000 for Western blotting (anti–claudin-1, anti-occludin, and anti-TfR). Rabbit anti-PKCζ (C-20; sc-216; 1:75) and mouse anti-CD63 (sc5275; 1:1000) were obtained from Santa Cruz Biotechnology (Santa Cruz, CA). Mouse anti-ubiquitin (recognizes mono- and polyubiquitinylated conjugates; clone FK2; 1:50) and rabbit anti–furin convertase (canine; 1:300) were purchased from Enzo Life Sciences (Plymouth Meeting, PA). Mouse anti-Tsg101 (4A10; ab83; 1:1000), rabbit anti-NUMB* (ab14140; 1:50), mouse anti–desmoglein-2 (ab14415; 1:25), and mouse anti-M6PR (ab2733; 1:200) were purchased from AbCam (Cambridge, UK). Mouse anti-EEA1 was purchased from BD Biosciences (610457; San Jose, CA; 1:100). Mouse anti–β-tubulin (T4026; 1:5000) was purchased from Sigma-Aldrich (St. Louis, MO). Mouse anti-GP135 (Ojakian and Schwimmer, 1988) was a kind gift from George Ojakian (SUNY Downstate Medical Center, Brooklyn, NY) and used at a dilution of 1:10. Mouse anti-LAMP1* (Developmental Studies Hybridoma Bank, University of Iowa, Iowa City, IA) was a kind gift from Scott Lawrence (University College, London, UK) and used at a dilution of 1:500. Species-specific fluorophore-conjugated anti–immunoglobulin G secondary antibodies (Alexa Fluor 488, 546, and 633 nm) were all purchased from Molecular Probes, and each was used at a dilution of 1:200 (Invitrogen, Carlsbad, CA). Goat anti–mouse-HRP–conjugated secondary antibody was obtained from Sigma-Aldrich and goat anti–rabbit-HRP was purchased from Pierce (Rockford, IL) and used at a 1:5000 dilution.

Generation of adenovirus

The generation of high-titer, purified adenoviruses using the Iowa RapAd system has been described previously (Anderson *et al.*, 2000). Briefly, Ad-expressing CHMP3$^{1–179}$GFP (Ad-CHMP3$^{1–179}$GFP) was prepared by subcloning the DNA construct into pacAd5 CMV K-N pA shuttle vector (a kind gift from Beverly Davidson, University of Iowa, Iowa City, IA). This was then digested with PacI alongside pacAd5 9.2–100 sub360 backbone vector and mixed and transfected according to manufacturer's instructions, into low-passage HEK293 cells using Lipofectamine 2000 (Invitrogen). Cells were left for 10 d to allow recombination between digested shuttle and backbone vectors and for visible cytopathic effects to be observed. Lysates were then collected and used for further bulking of the virus. Ad vectors were then grown to high titer and purified using CsCl gradient methods, as previously described (Anderson *et al.*, 2000; Caunt and McArdle, 2010).

Cell culture, transfections, and transduction

MDCKII cells (Madin-Darby canine kidney cells; #00062107; European Collection of Cell Cultures, Salisbury, UK) and 16HBE14o- (human bronchial epithelial cells; a kind gift from Dieter Gruenert, University of California–San Francisco, San Francisco, CA; Cozens *et al.*, 1994) were maintained at 37°C and 5% CO_2 in DMEM supplemented with 10% (vol/vol) fetal bovine serum (FBS), 2 mM L-glutamine, 100 U/ml penicillin, and 100 μg/ml streptomycin. CaCo-2 cells (#86010202; ECACC) were similarly maintained, except for the addition of 20% (vol/vol) FBS, 1x nonessential amino acids and 10 mM HEPES. All cell media and supplements were purchased from Lonza (Basel, Switzerland). Cells were tested for mycoplasma contamination using MycoAlert (Lonza). Cells were plated onto 13-mm coverslips in 24-well plates (Nunc, Roskilde, Denmark) and grown until ~80–90% confluent, at which time they were transfected with Lipofectamine 2000 (Invitrogen) according to the manufacturer's instructions.

Immunofluorescence

At 24 h posttransfection, cells were fixed with 4% (wt/vol) paraformaldehyde fixation buffer (PFA) in phosphate-buffered saline (PBS) for 20 min and permeabilized in methanol cooled to −20°C for 5 min. Cells stained with antibodies indicated by an asterisk (see *Antibodies and DNA constructs*) were fixed and permeabilized with methanol cooled to −20°C for 10 min. Cells were then blocked with 10% (vol/vol) FBS in PBS for 30 min. Primary and secondary antibodies were diluted in 2% FBS-PBS (2% FBS in PBS), and cells were incubated with primary antibodies for 2 h at 18°C and with secondary antibodies for 1 h. Cells were washed five times for 5 min (per wash) with 2% FBS-PBS following all antibody incubations. Stained cells were then mounted in Mowiol (Calbiochem, San Diego, CA) containing DAPI (Sigma-Aldrich) and examined on a Zeiss LSM510META laser-scanning confocal microscope with images taken.

siRNA knockdowns

siRNA oligonucleotides and reagents were purchased from Dharmacon (Thermo Fisher Scientific, Lafayette, CO). Tsg101 was depleted using ON-TARGETplus individual siRNA duplex (CCGUUUAGAUCAAGAAGUA; J-003549-06). As a control, ON-TARGETplus Non-targeting siRNA was used. CaCo-2 cells were plated at high density into either six-well plates (for Western blotting; Nunc), or onto 13-mm glass coverslips (for immunofluorescence), and incubated with complete CaCo-2 growth media (lacking antibiotics) at 37°C, 5% CO_2 for ~4 h to adhere. Cells were transfected with 100 nM of siRNA using DharmaFECT 1 transfection reagent according to the manufacturer's instructions and incubated at 37°C, 5% CO_2 for the desired time period, with media changed after 3 d.

Endocytosis and recycling biotin assays

The biotinylation assay to study endocytosis and recycling of tight junction proteins was modified from a method described previously (Nishimura and Sasaki, 2008). Confluent cells plated on to 35-mm dishes were transferred to ice and washed with PBS supplemented with 0.9 mM $CaCl_2$ and 0.33 mM $MgCl_2$ (PBS-CM). Cells were then incubated with the cleavable non-membrane-permeable sulfo-NHS-SS-biotin (Pierce; in PBS-CM) at a concentration of 0.5 mg/ml for 30 min on ice. Free biotin was then quenched using 50 mM NH_4Cl (in PBS-CM) for 15 min (4°C). For the endocytosis assay, prewarmed complete growth medium was added, and cells were returned to 37°C for indicated times. Cells were then transferred to ice to stop endocytosis, and surface (nonendocytosed) biotin was stripped by reduction with 100 mM 2-mercaptoethanesulfonate (MESNA) in Tris-buffered saline supplemented with calcium and magnesium (TBS-CM) for three 10-min treatments (on ice). Internalized biotinylated cargo was protected from biotin stripping with MESNA by an intact membrane. Free –SH groups were then quenched by incubating cells

with 5 mg/ml iodoacetamide (in PBS-CM) three times for 5 min each time.

For the recycling assay, this process was repeated with 20-min incubations at 37°C in complete growth medium. To control for potential loss of biotinylated cargo via degradation, a recycling condition was included that lacked the second MESNA treatment. Thus any loss in biotinylated cargo at this step, relative to the endocytosis step, would indicate a loss in signal due to degradation of cargo instead of recycling. Cells were lysed (1.25% [vol/vol] Triton X-100, 0.25% [wt/vol] SDS, 50 mM Tris-HCl, pH 8.0, 150 mM NaCl, 5 mM EDTA, 5 mg/ml iodoacetamide, 10 µg/ml APMSF) on ice, pulse-sonicated, and centrifuged at 15,000 × *g* to remove large/nuclear debris. An equal volume of the postnuclear supernatant was taken from each sample for use as a loading control. Biotinylated proteins were collected by incubation with Neutravidin beads (Pierce), rotating overnight at 4°C. Beads were then washed by centrifuging at 1000 × *g*, five times with wash buffer (0.5% [vol/vol] Triton X-100, 0.1% [wt/vol] SDS, 50 mM Tris-HCl, pH 8.0, 150 mM NaCl, 5 mM EDTA) and 3 times with PBS-CM. Reducing sample buffer was then added to each sample to release biotinylated proteins from the beads and, following boiling, samples were loaded onto a 15% Tris-glycine SDS–PAGE gel. Separated proteins were transferred to nitrocellulose and immunoblotted for the protein indicated. Signals were detected by enhanced chemiluminescence or Chemiglow West Chemiluminescence Substrate (Alpha Innotech, San Leandro, CA) and quantified using an Optichem detector with associated software (Ultra Violet Products, Cambridge, UK). For quantification of the biotinylated proteins, the amount of claudin-1 and occludin was normalized to their respective total protein bands, determined from nonisolated lysate samples. Where results were plotted graphically (Prism; GraphPad, La Jolla, CA), values were expressed as a percentage of the total claudin-1 or occludin biotinylated at the surface. For recycling assays using Ad-CHMP3$^{1–179}$GFP infections, MDCKII cells were allowed to grow past confluency on 35-mm dishes, and then infected with Ad-CHMP3$^{1–179}$GFP for 16 h and subsequently surface-biotinylated. The recycling assay was then performed as described previously.

Caco-2 TER measurements

CaCo-2 cells were plated into six-well Nunc plates and transfected with ON-TARGETplus Non-targeting siRNA or Tsg101 siRNA, as detailed previously. Cells were incubated at 37°C, 5% CO_2 for 3 d. Cells were washed in PBS, trypsinized, and resuspended in CaCo-2 growth media. Cells were plated in triplicate on Transwell (#3470; Corning Life Sciences, Corning, NY) permeable polyester filters (0.4-µm pore size, 0.33-cm^2 surface area) at 2.5×10^5 cells/filter and incubated at 37°C, 5% CO_2. TER was measured every 24 h for 4 d using a EVOM TER machine with an Endohm-6 chamber (World Precision Instruments, Sarasota, FL), with media changed after every reading.

CaCo-2 three-dimensional cyst culture and immunofluorescence

CaCo-2 cells were plated into six-well Nunc plates and transfected with ON-TARGETplus Non-targeting siRNA or Tsg101 siRNA, as detailed previously. Cells were incubated at 37°C, 5% CO_2 for 3 d. Cells were washed in PBS, trypsinized and resuspended in antibiotic-free CaCo-2 growth media. A cell:matrix mix was prepared containing 5.8×10^4 CaCo-2 cells/ml, 0.02 M HEPES (pH 7.4), 1 mg/ml Collagen I (Inamed Biomaterials, Fremont, CA), and 40% Growth Factor Reduced BD Matrigel Matrix (BD Biosciences). The cell:matrix mix was plated into an eight-chamber slide, incubated at 37°C, 5% CO_2 for 1 h to solidify, and overlaid with antibiotic-free CaCo-2 growth medium. Cysts were allowed to develop for 10 d at 37°C, 5% CO_2, with media changed every 3–4 d. After a 10-d culture, cysts were washed in PBS, treated with 5U/ml Collagenase VII (Sigma-Aldrich) for 15 min, and fixed in 4% (wt/vol) PFA for 30 min at room temperature. Cysts were washed three times for 20 min with 1X wash buffer (10X stock, pH 7.4: 1.3 M sodium chloride, 70 mM dibasic heptahydrate sodium phosphate, 30 mM monobasic monohydrate sodium phosphate, 77 mM sodium azide, 1% [wt/vol] BSA, 2% [vol/vol] Triton-X 100, 0.4% [vol/vol] Tween-20; all Sigma-Aldrich). Cysts were incubated with blocking buffer (10% [vol/vol] FBS in 1X wash buffer) for 1 h at room temperature, and the incubated with primary antibodies diluted in blocking buffer overnight at 4°C. Cysts were washed three times for 20 min with 1X wash buffer and incubated with secondary antibodies diluted in blocking buffer for 1 h at room temperature. After a further three 20-min washes with 1X wash buffer, cysts were rinsed twice in PBS and postfixed in 4% (wt/vol) PFA for 30 min at room temperature. Cysts were washed three times for 5 min with PBS and incubated with DAPI (4 µg/ml) for 30 min at room temperature to stain the nuclei. After a final rinse in PBS, cysts were mounted in Mowiol (Calbiochem) and examined on a Zeiss LSM510 META laser-scanning confocal microscope (Welwyn Garden City, UK).

ACKNOWLEDGMENTS

Dieter Gruenert, University of California–San Francisco, kindly provided the 16-HBE cells. The GP135 antibody was a gift from George Ojakian, SUNY Downstate Medical Center; EEA1 from Michael Clague, University of Liverpool, Liverpool, UK; and LAMP1 from Scott Lawrence, University College, London, UK. The pacAd5 CMV K-N pA shuttle vector was a gift from Beverly Davidson, University of Iowa, Iowa City, IA. Confocal microscopy was carried out in the University of Bath Bioimaging Suite, and we appreciate help received from Adrian Rogers. This work was supported by a Cancer Research UK project grant (C26932/A9548). Preliminary experiments were funded by Wellcome Trust (project grant 070085 to PW). A.D.C. was supported by an RCUK Academic Fellowship and L.F. by a BBSRC PhD studentship.

REFERENCES

Anderson RD, Haskell RE, Xia H, Roessler BJ, Davidson BL (2000). A simple method for the rapid generation of recombinant adenovirus vectors. Gene Ther 7, 1034–1038.

Babst M, Odorizzi G, Estepa EJ, Emr SD (2000). Mammalian tumor susceptibility gene 101 (TSG101) and the yeast homologue, Vps23p, both function in late endosomal trafficking. Traffic 1, 248–258.

Baldys A, Raymond JR (2009). Critical role of ESCRT machinery in EGFR recycling. Biochemistry 48, 9321–9323.

Bishop N, Woodman P (2000). ATPase-defective mammalian VPS4 localizes to aberrant endosomes and impairs cholesterol trafficking. Mol Biol Cell 11, 227–239.

Brennan K, Offiah G, McSherry EA, Hopkins AM (2010). Tight junctions: a barrier to the initiation and progression of breast cancer. J Biomed Biotechnol 2010, 460607.

Bryant DM, Mostov KE (2008). From cells to organs: building polarized tissue. Nat Rev Mol Cell Biol 9, 887–901.

Capaldo CT, Nusrat A (2009). Cytokine regulation of tight junctions. Biochim Biophys Acta 1788, 864–871.

Carlton JG, Martin-Serrano J (2007). Parallels between cytokinesis and retroviral budding: a role for the ESCRT machinery. Science 316, 1908–1912.

Caunt CJ, McArdle CA (2010). Stimulus-induced uncoupling of extracellular signal-regulated kinase phosphorylation from nuclear localization is dependent on docking domain interactions. J Cell Sci 123, 4310–4320.

Chalmers AD, Lachani K, Shin Y, Sherwood V, Cho KW, Papalopulu N (2006). Grainyhead-like 3, a transcription factor identified in a microarray screen, promotes the specification of the superficial layer of the embryonic epidermis. Mech Dev 123, 702–718.

Cozens AL, Yezzi MJ, Kunzelmann K, Ohrui T, Chin L, Eng K, Finkbeiner WE, Widdicombe JH, Gruenert DC (1994). CFTR expression and chloride secretion in polarized immortal human bronchial epithelial cells. Am J Respir Cell Mol Biol 10, 38–47.

Doyotte A, Russell MR, Hopkins CR, Woodman PG (2005). Depletion of TSG101 forms a mammalian "Class E" compartment: a multicisternal early endosome with multiple sorting defects. J Cell Sci 118, 3003–3017.

Dukes JD, Richardson JD, Simmons R, Whitley P (2008). A dominant-negative ESCRT-III protein perturbs cytokinesis and trafficking to lysosomes. Biochem J 411, 233–239.

Fujita H, Yamanaka M, Imamura K, Tanaka Y, Nara A, Yoshimori T, Yokota S, Himeno M (2003). A dominant negative form of the AAA ATPase SKD1/VPS4 impairs membrane trafficking out of endosomal/lysosomal compartments: class E vps phenotype in mammalian cells. J Cell Sci 116, 401–414.

Fujita Y, Krause G, Scheffner M, Zechner D, Leddy HE, Behrens J, Sommer T, Birchmeier W (2002). Hakai, a c-Cbl-like protein, ubiquitinates and induces endocytosis of the E-cadherin complex. Nat Cell Biol 4, 222–231.

Furuse M, Hata M, Furuse K, Yoshida Y, Haratake A, Sugitani Y, Noda T, Kubo A, Tsukita S (2002). Claudin-based tight junctions are crucial for the mammalian epidermal barrier: a lesson from claudin-1-deficient mice. J Cell Biol 156, 1099–1111.

Garrus JE *et al.* (2001). Tsg101 and the vacuolar protein sorting pathway are essential for HIV-1 budding. Cell 107, 55–65.

Getsios S, Huen AC, Green KJ (2004). Working out the strength and flexibility of desmosomes. Nat Rev Mol Cell Biol 5, 271–281.

Goldstein B, Macara IG (2007). The PAR proteins: fundamental players in animal cell polarization. Dev Cell 13, 609–622.

Grant BD, Donaldson JG (2009). Pathways and mechanisms of endocytic recycling. Nat Rev Mol Cell Biol 10, 597–608.

Hanahan D, Weinberg RA (2000). The hallmarks of cancer. Cell 100, 57–70.

Herz HM, Chen Z, Scherr H, Lackey M, Bolduc C, Bergmann A (2006). *vps25* mosaics display non-autonomous cell survival and overgrowth, and autonomous apoptosis. Development 133, 1871–1880.

Herz HM, Woodfield SE, Chen Z, Bolduc C, Bergmann A (2009). Common and distinct genetic properties of ESCRT-II components in *Drosophila*. PLoS One 4, e4165.

Hopkins AM, Walsh SV, Verkade P, Boquet P, Nusrat A (2003). Constitutive activation of Rho proteins by CNF-1 influences tight junction structure and epithelial barrier function. J Cell Sci 116, 725–742.

Hurley JH, Emr SD (2006). The ESCRT complexes: structure and mechanism of a membrane-trafficking network. Annu Rev Biophys Biomol Struct 35, 277–298.

Ikari A, Takiguchi A, Atomi K, Sugatani J (2010). Epidermal growth factor increases clathrin-dependent endocytosis and degradation of claudin-2 protein in MDCK II cells. J Cell Physiol 226, 2448–2456.

Ivanov AI, Nusrat A, Parkos CA (2005). Endocytosis of the apical junctional complex: mechanisms and possible roles in regulation of epithelial barriers. Bioessays 27, 356–365.

Leithe E, Kjenseth A, Sirnes S, Stenmark H, Brech A, Rivedal E (2009). Ubiquitylation of the gap junction protein connexin-43 signals its trafficking from early endosomes to lysosomes in a process mediated by Hrs and Tsg101. J Cell Sci 122, 3883–3893.

Leung SM, Ruiz WG, Apodaca G (2000). Sorting of membrane and fluid at the apical pole of polarized Madin-Darby canine kidney cells. Mol Biol Cell 11, 2131–2150.

Li J, Belogortseva N, Porter D, Park M (2008). Chmp1A functions as a novel tumor suppressor gene in human embryonic kidney and ductal pancreatic tumor cells. Cell Cycle 7, 2886–2893.

Li L, Cohen SN (1996). *tsg101*: a novel tumor susceptibility gene isolated by controlled homozygous functional knockout of allelic loci in mammalian cells. Cell 85, 319–329.

Liu RT, Huang CC, You HL, Chou FF, Hu CC, Chao FP, Chen CM, Cheng JT (2002). Overexpression of tumor susceptibility gene *TSG101* in human papillary thyroid carcinomas. Oncogene 21, 4830–4837.

Lobert VH, Brech A, Pedersen NM, Wesche J, Oppelt A, Malerod L, Stenmark H (2010). Ubiquitination of α5β1 integrin controls fibroblast migration through lysosomal degradation of fibronectin-integrin complexes. Dev Cell 19, 148–159.

Malerod L, Stuffers S, Brech A, Stenmark H (2007). Vps22/EAP30 in ESCRT-II mediates endosomal sorting of growth factor and chemokine receptors destined for lysosomal degradation. Traffic 8, 1617–1629.

Martin-Belmonte F, Mostov K (2008). Regulation of cell polarity during epithelial morphogenesis. Curr Opin Cell Biol 20, 227–234.

Martin-Serrano J, Zang T, Bieniasz PD (2003). Role of ESCRT-I in retroviral budding. J Virol 77, 4794–4804.

Matsuda M, Kubo A, Furuse M, Tsukita S (2004). A peculiar internalization of claudins, tight junction-specific adhesion molecules, during the intercellular movement of epithelial cells. J Cell Sci 117, 1247–1257.

Moberg KH, Schelble S, Burdick SK, Hariharan IK (2005). Mutations in *erupted*, the *Drosophila* ortholog of mammalian tumor susceptibility gene 101, elicit non-cell-autonomous overgrowth. Dev Cell 9, 699–710.

Morimoto S, Nishimura N, Terai T, Manabe S, Yamamoto Y, Shinahara W, Miyake H, Tashiro S, Shimada M, Sasaki T (2005). Rab13 mediates the continuous endocytic recycling of occludin to the cell surface. J Biol Chem 280, 2220–2228.

Niessen CM, Gottardi CJ (2008). Molecular components of the adherens junction. Biochim Biophys Acta 1778, 562–571.

Nishimura N, Sasaki T (2008). Cell-surface biotinylation to study endocytosis and recycling of occludin. Methods Mol Biol 440, 89–96.

Oh KB, Stanton MJ, West WW, Todd GL, Wagner KU (2007). Tsg101 is upregulated in a subset of invasive human breast cancers and its targeted overexpression in transgenic mice reveals weak oncogenic properties for mammary cancer initiation. Oncogene 26, 5950–5959.

Ojakian GK, Schwimmer R (1988). The polarized distribution of an apical cell surface glycoprotein is maintained by interactions with the cytoskeleton of Madin-Darby canine kidney cells. J Cell Biol 107, 2377–2387.

Palacios F, Tushir JS, Fujita Y, D'Souza-Schorey C (2005). Lysosomal targeting of E-cadherin: a unique mechanism for the down-regulation of cell-cell adhesion during epithelial to mesenchymal transitions. Mol Cell Biol 25, 389–402.

Rahner C, Mitic LL, Anderson JM (2001). Heterogeneity in expression and subcellular localization of claudins 2, 3, 4, and 5 in the rat liver, pancreas, and gut. Gastroenterology 120, 411–422.

Raiborg C, Malerod L, Pedersen NM, Stenmark H (2008). Differential functions of Hrs and ESCRT proteins in endocytic membrane trafficking. Exp Cell Res 314, 801–813.

Raiborg C, Stenmark H (2009). The ESCRT machinery in endosomal sorting of ubiquitylated membrane proteins. Nature 458, 445–452.

Raleigh DR *et al.* (2011). Occludin S408 phosphorylation regulates tight junction protein interactions and barrier function. J Cell Biol 193, 565–582.

Razi M, Futter CE (2006). Distinct roles for Tsg101 and Hrs in multivesicular body formation and inward vesiculation. Mol Biol Cell 17, 3469–3483.

Rodahl LM, Haglund K, Sem-Jacobsen C, Wendler F, Vincent JP, Lindmo K, Rusten TE, Stenmark H (2009). Disruption of Vps4 and JNK function in Drosophila causes tumour growth. PLoS One 4, e4354.

Ruland J, Sirard C, Elia A, MacPherson D, Wakeham A, Li L, de la Pompa JL, Cohen SN, Mak TW (2001). p53 accumulation, defective cell proliferation, and early embryonic lethality in mice lacking *tsg101*. Proc Natl Acad Sci USA 98, 1859–1864.

Rusten TE, Filimonenko M, Rodahl LM, Stenmark H, Simonsen A (2007). ESCRTing autophagic clearance of aggregating proteins. Autophagy 4, 233–236.

Shen L, Turner JR (2008). Intercellular junctions: actin the PARt. Curr Biol 18, R1014–R1017.

Shen L, Weber CR, Turner JR (2008). The tight junction protein complex undergoes rapid and continuous molecular remodeling at steady state. J Cell Biol 181, 683–695.

Shim S, Kimpler LA, Hanson PI (2007). Structure/function analysis of four core ESCRT-III proteins reveals common regulatory role for extreme C-terminal domain. Traffic 8, 1068–1079.

Shin K, Fogg VC, Margolis B (2006). Tight junctions and cell polarity. Annu Rev Cell Dev Biol 22, 207–235.

Shivas JM, Morrison HA, Bilder D, Skop AR (2010). Polarity and endocytosis: reciprocal regulation. Trends Cell Biol 20, 445–452.

Steed E, Balda MS, Matter K (2010). Dynamics and functions of tight junctions. Trends Cell Biol 20, 142–149.

Suzuki A, Ohno S (2006). The PAR-aPKC system: lessons in polarity. J Cell Sci 119, 979–987.

Takahashi S, Iwamoto N, Sasaki H, Ohashi M, Oda Y, Tsukita S, Furuse M (2009). The E3 ubiquitin ligase LNX1p80 promotes the removal of claudins from tight junctions in MDCK cells. J Cell Sci 122, 985–994.

Thompson BJ, Mathieu J, Sung HH, Loeser E, Rorth P, Cohen SM (2005). Tumor suppressor properties of the ESCRT-II complex component Vps25 in *Drosophila*. Dev Cell 9, 711–720.

Toyoshima M, Tanaka N, Aoki J, Tanaka Y, Murata K, Kyuuma M, Kobayashi H, Ishii N, Yaegashi N, Sugamura K (2007). Inhibition of tumor growth and metastasis by depletion of vesicular sorting protein Hrs: its regulatory role on E-cadherin and β-catenin. Cancer Res 67, 5162–5171.

Traweger A, Fang D, Liu YC, Stelzhammer W, Krizbai IA, Fresser F, Bauer HC, Bauer H (2002). The tight junction-specific protein occludin is a

functional target of the E3 ubiquitin-protein ligase itch. J Biol Chem 277, 10201–10208.
Vaccari T, Bilder D (2005). The *Drosophila* tumor suppressor *vps25* prevents nonautonomous overproliferation by regulating Notch trafficking. Dev Cell 9, 687–698.
Vaccari T, Bilder D (2009). At the crossroads of polarity, proliferation and apoptosis: the use of Drosophila to unravel the multifaceted role of endocytosis in tumor suppression. Mol Oncol 3, 354–365.
Vaccari T, Rusten TE, Menut L, Nezis IP, Brech A, Stenmark H, Bilder D (2009). Comparative analysis of ESCRT-I, ESCRT-II and ESCRT-III function in *Drosophila* by efficient isolation of ESCRT mutants. J Cell Sci 122, 2413–2423.
Van Itallie CM, Anderson JM (2006). Claudins and epithelial paracellular transport. Annu Rev Physiol 68, 403–429.
Van Itallie CM, Fanning AS, Anderson JM (2003). Reversal of charge selectivity in cation or anion-selective epithelial lines by expression of different claudins. Am J Physiol Renal Physiol 285, F1078–F1084.
Vogelmann R, Nelson WJ (2005). Fractionation of the epithelial apical junctional complex: reassessment of protein distributions in different substructures. Mol Biol Cell 16, 701–716.
Wagner KU, Krempler A, Qi Y, Park K, Henry MD, Triplett AA, Riedlinger G, Rucker IE, Hennighausen L (2003). Tsg101 is essential for cell growth, proliferation, and cell survival of embryonic and adult tissues. Mol Cell Biol 23, 150–162.
Whitley P, Reaves BJ, Hashimoto M, Riley AM, Potter BV, Holman GD (2003). Identification of mammalian Vps24p as an effector of phosphatidylinositol 3,5-bisphosphate-dependent endosome compartmentalization. J Biol Chem 278, 38786–38795.
Woodman P (2009). ESCRT proteins, endosome organization and mitogenic receptor down-regulation. Biochem Soc Trans 37, 146–150.
Xu Z, Liang L, Wang H, Li T, Zhao M (2003). HCRP1, a novel gene that is downregulated in hepatocellular carcinoma, encodes a growth-inhibitory protein. Biochem Biophys Res Commun 311, 1057–1066.
Yamamura R, Nishimura N, Nakatsuji H, Arase S, Sasaki T (2008). The interaction of JRAB/MICAL-L2 with Rab8 and Rab13 coordinates the assembly of tight junctions and adherens junctions. Mol Biol Cell 19, 971–983.
Yang J, Weinberg RA (2008). Epithelial-mesenchymal transition: at the crossroads of development and tumor metastasis. Dev Cell 14, 818–829.
Yoshimori T, Yamagata F, Yamamoto A, Mizushima N, Kabeya Y, Nara A, Miwako I, Ohashi M, Ohsumi M, Ohsumi Y (2000). The mouse SKD1, a homologue of yeast Vps4p, is required for normal endosomal trafficking and morphology in mammalian cells. Mol Biol Cell 11, 747–763.
Young TW, Rosen DG, Mei FC, Li N, Liu J, Wang XF, Cheng X (2007). Up-regulation of tumor susceptibility gene 101 conveys poor prognosis through suppression of p21 expression in ovarian cancer. Clin Cancer Res 13, 3848–3854.
Yu D, Turner JR (2008). Stimulus-induced reorganization of tight junction structure: the role of membrane traffic. Biochim Biophys Acta 1778, 709–716.
Zamborlini A, Usami Y, Radoshitzky SR, Popova E, Palu G, Gottlinger H (2006). Release of autoinhibition converts ESCRT-III components into potent inhibitors of HIV-1 budding. Proc Natl Acad Sci USA 103, 19140–19145.